We are IntechOpen, the world's leading publisher of Open Access books Built by scientists, for scientists

4,800
Open access books available

122,000
International authors and editors

135M
Downloads

Our authors are among the

154
Countries delivered to

TOP 1%
most cited scientists

12.2%
Contributors from top 500 universities

CLARIVATE ANALYTICS BOOK CITATION INDEX INDEXED

WEB OF SCIENCE™

Selection of our books indexed in the Book Citation Index in Web of Science™ Core Collection (BKCI)

Interested in publishing with us?
Contact book.department@intechopen.com

Numbers displayed above are based on latest data collected.
For more information visit www.intechopen.com

20

Working Fluid Selection for Low Temperature Solar Thermal Power Generation with Two-stage Collectors and Heat Storage Units

Pei Gang, Li Jing, Ji Jie
Department of Thermal Science and Energy Engineering, University of Science and Technology of China, Jinzhai Road 96#, Hefei City, Anhui Province, People's Republic of China

1. Introduction

Organic Rankine Cycle (ORC) is named for its use of an organic, high molecular mass fluid that boils at a lower temperature than the water. Among many well-proven technologies, the ORC is one of the most favorable and promising ways for low-temperature applications. In comparison to water, organic fluids are advantageous when the plant runs at low temperature or low power. The ORC is scalable to smaller unit sizes and higher efficiencies during cooler ambient temperatures, immune from freezing at cold winter nighttime temperatures, and adaptable for conducting semi-attended or unattended operations [1]. Simpler and cheaper turbine can be used due to the limited volume ratio of organic fluid at the turbine outlet and inlet [2]. In the case of a dry fluid, ORC can be employed at lower temperatures without requiring superheating. This results in a practical increase in efficiency over the use of the cycle with water as the working fluid [3]. ORC can be easily modularized and utilized in conjunction with various heat sources. The success of the ORC technology is reinforced by high technological maturity of majority of its components, spurred by extensive use in refrigeration applications [4]. Moreover, electricity generation near the point of use will lead to smaller-scale power plants, and thus the ORC is particularly suitable for off-grid generation.

The selection of the working fluid is of key importance in ORC applications. This is because the fluid must have not only thermophysical properties that match the application but also adequate chemical stability at the desired working temperature. There are several optimal characteristics of the working fluid:

1. Dry or isentropic fluid to avoid superheating at the turbine inlet, for the sake of an acceptable cycle efficiency;
2. Chemical stability to prevent deteriorations and decomposition at operating temperatures;
3. Non-fouling, non-corrosiveness, non-toxicity and non-flammability;
4. Good availability and low cost.

However, not all the desired general requirements can be satisfied in a practical ORC. In the previous research, numerous theoretical and experimental studies have focused on ORC fluid selection with special respect to thermodynamic properties. Hung et al. studied waste

heat recovery of ORC using dry fluids. The results revealed that irreversibility depended on the type of heat source. Working fluid of the lowest irreversibility in recovering high-temperature waste heat fails to perform favorably in recovering low-temperature waste heat [5]. Liu et al. presented a performance analysis of ORC subjected to the influence of working fluid. It was revealed that thermal efficiency for various working fluids is a weak function of critical temperature [6]. Saleh et al. conducted a thermodynamic screening of 31 pure component working fluids for ORC using Backone equation of state. It was suggested that should the vapor leaving the turbine be superheated, an internal heat exchanger may be employed [7]. Madhawa et al. presented a cost-effective optimum design criterion for ORC utilizing low-temperature geothermal heat sources. Results indicated that ammonia possesses minimum objective function because of a better heat transfer performance, but not necessarily a maximum cycle efficiency [8]. Drescher et al. proposed a new heat transfer configuration with two thermal oil cycles to avoid the constriction of the pinch point between the organic fluid and thermal oil at the beginning of vaporization in biomass power and heat plants. Based on the new design, the influence of working fluids was analyzed and the family of alkyl benzenes showed highest efficiencies [9].

It should be noted that the majority of the previous research on ORC fluid selection was concerned in fields of waste heat recovery, geothermal and biomass applications. Integration of ORC and solar collectors has attracted limited attention. Wang et al. designed, constructed, and tested a prototype low-temperature solar Rankine system. With a 1.73 kW rolling-piston expander overall power generation efficiency is estimated at 4.2% or 3.2% for evacuated or flat plate collectors (FPC) respectively [10]. Ormat supplied a 1 MW power plant, based on ORC technology, to the new power facility of Arizona Public Service. It represented the first parabolic trough plant constructed since 1991 [11].

This paper combines ORC with compound parabolic concentrator (CPC). The feasibility and advantage of CPC application in solar thermal electric generation have been outlined [12, 13, 14]. In particular, FPCs are employed in series with CPC collectors. Three considerations should be made to understand the advantage of two-stage collectors. First, although CPC collectors offer relatively low overall heat loss when operated at high temperatures, efficiency may be lower than that of FPCs in low temperature ranges. Reflectivity of CPC reflectors and difference between the inner and outer diagram of the evacuated tube result in lower intercept efficiency. Thus, overall collector efficiency may be improved when FPCs are employed to preheat the working fluid prior to entering a field of higher-temperature CPC collectors. Second, FPC can absorb energy originating from all directions above the absorber (both beam and diffuse solar irradiance). Third, FPC currently costs less than CPC collector. Part of the reason is that production of FPC is considerably larger. Many excellent models of FPC are available commercially for solar designers [15]. Similarly, collector efficiency may be improved when two-stage heat storage units are employed with phase change material (PCM) of a lower melting point as the first stage, and PCM of a higher melting point as the second stage. Details are provided in the sections below.

Due this innovative design the working fluid selection criteria are different from that for a solo ORC or ORC plants in waste heat recovery, geothermal and biomass fields. The collector efficiency will be influenced directly by the thermophysical properties of the working fluid e.g. the enthalpy-temperature diagram in the isobaric heating process. Furthermore, the optimal proportion of FPC area to overall collector area for the two-stage collectors is determined by both the operation condition and selection of working fluid.

The low-temperature solar thermal electric generation with two-stage collectors and heat storage units is first designed. Subsequently, fundamentals of heat transfer and thermodynamics are illustrated. A mathematical model is established and a numerical simulation is carried out. Five widely or newly used fluids are considered in this study. The influences of working fluids on heat collection, ORC and global electricity efficiency are investigated. Performance comparison among R113, R123, R245fa, pentane and butane is presented.

2. Design and fundamentals

Figure 1 presents the diagram of low-temperature solar thermal electric generation with two-stage collectors and heat storage units. The system consists of FPC and CPC collectors, heat storage, and ORC subsystem. FPCs offer the advantage of accepting high pressure without leakage. The organic fluid flows through FPCs directly and is heated indirectly by CPC collectors with the intermediate of conduction oil. The ORC subsystem consists of evaporator (E), organic fluid/heat storage tank with PCM, turbine (T), generator (G), regenerator (R), condenser, and pumps. The first-stage heat storage is filled with PCM (1), while the second heat storage is filled with PCM (2). Melting point of PCM (1) is lower than that of PCM (2).

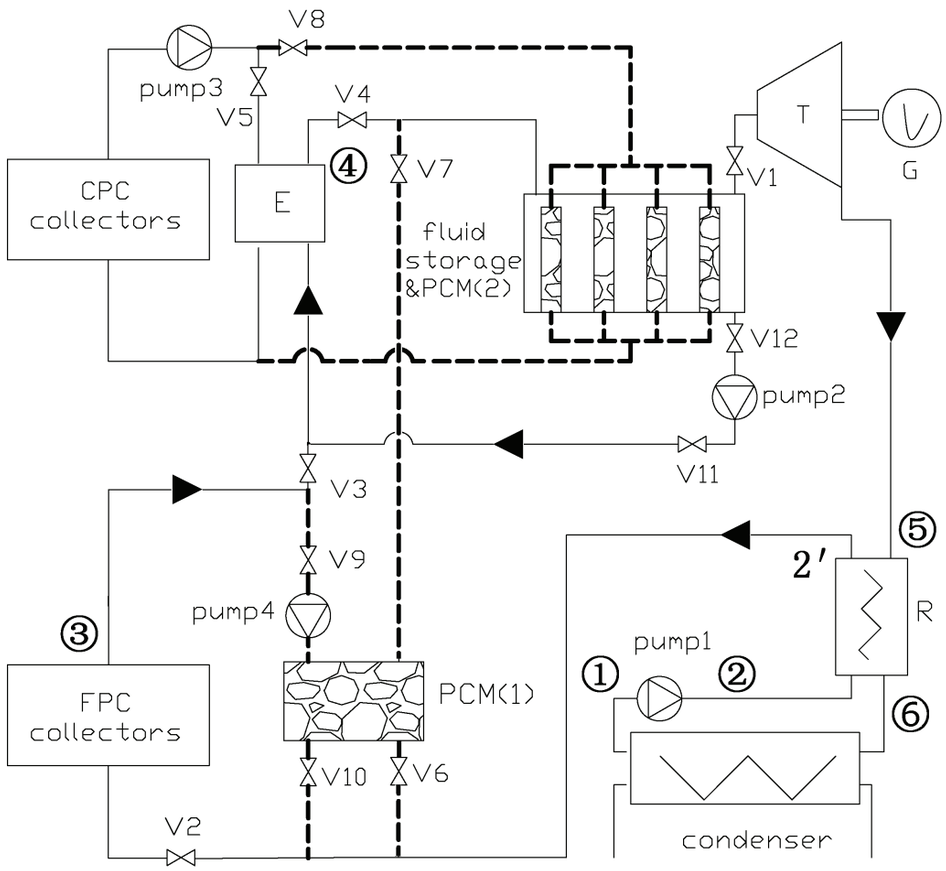

Fig. 1. Low-temperature solar thermal electric generation with two-stage collectors and heat storage units

There are three basic modes of the low-temperature solar thermal electricity system in the practical operating period. In Mode I, the system requires generation of electricity and irradiation is available. In this mode, Valves 1, 2, 3, 4, and 5 are open. Pumps 1 and 3 are running. Valves 11 and 12 may be open while Pump 2 may run to prevent superheating in the evaporator when irradiation is strong. Flow direction of the organic fluid is illustrated by arrows. Organic fluid is preheated in FPCs and subsequently vaporized in the evaporator under high pressure. In the event that organic fluid is not totally vaporized, liquid will drop into the fluid storage tank; it will not harm the turbine. Vapor flows into the turbine and expands, exporting power in the process because of enthalpy drop. The outlet vapor is cooled down in the regenerator and condensed to a liquid state in the condenser. Meanwhile, the liquid is pressurized by Pump 1 and warmed in the regenerator. Subsequently, organic fluid is sent back to the first stage collectors and is circulated. On the use of Pump 2, the system can run steadily in a wide irradiation range. Without any complicated controlling device, the process of heat storage or heat release can occur while electricity is being generated.

In Mode II, the system does not require generation of electricity but irradiation is sound. Valves 2, 8, 9, and 10 are open. Pumps 3 and 4 are running. The dashed lines in Fig.1 represent pipes for heat storage, with the exception of the line that passes through Valves 6 and 7. FPCs are connected with PCM (1) and CPC collectors are connected with PCM (2).

In Mode III, the system requires generation of electricity; however, irradiation is either extremely weak or unavailable. Valves 1, 6, and 7 are open, and Pump 1 is running. Organic fluid is preheated by the first-stage heat storage of PCM (1) and further heated by the second-stage heat storage of PCM (2).

Mode I is described as the simultaneous processes of heat collection and power conversion and is under special investigation in this work.

3. Working fluid properties

The ORC fluid can be classified into three categories according to the temperature-entropy $(T-s)$ diagrams. It is noteworthy that for some kinds of fluids, the derivative of temperature with respect to entropy on the saturation vapor curve may change from positive value to negative value, e.g. $\frac{dT}{ds}$ of R123 on the saturation vapor curve is positive when T is smaller than 150°C while negative at higher temperature ranges. In this case, dry fluids are generally named for the positive $\frac{dT}{ds}$ in practical operation temperature range from the cold side to the hot side. And wet fluids would have negative $\frac{dT}{ds}$ on the saturation vapor curve. Meanwhile, isentropic fluids have approximately infinite value of $\frac{dT}{ds}$ (nearly vertical curve).

The working fluids of dry or isentropic type are more appropriate for ORC systems. The reason is that dry or isentropic fluids are superheated after isentropic expansion, thereby eliminating the concerns of impingement of liquid droplets on the turbine blades and making the superheated apparatus unnecessary [6]. Based on this consideration, five dry fluids are selected in the analysis. They are R113, R123, R245fa, pentane and butane. Some of properties of these fluids are listed in table 1. The optimal FPC proportion and the overall collector efficiency are related to the latent heat and heat capacity in saturation liquid states as discussed in Section 5.3.

	R123	R113	R245fa	pentane	butane
Critical pressure /Mpa	3.66	3.39	3.65	3.37	3.79
Critical temperature /°C	183.7	214.1	154.1	196.6	152.0
Boiling point /°C	27.8	47.5	15.1	36.1	-0.5
Latent heat, 120/°C kJ/kg	120.52	116.61	111.77	271.13	213.35
Heat capacity in saturation liquid state, $kJ/(kg\cdot$°C)	1.20	1.04	1.78	2.91	3.52

Table 1. Thermodynamic properties of the working fluids

4. Thermodynamics and heat transfer

4.1 Calculation of thermodynamic cycle

Figure 2 presents the scheme of thermodynamic cycle of a typical dry fluid. Point 1 illustrates the state of fluid at the condenser outlet; Point 2 at the Pump 1 outlet; Point 2′ at the regenerator outlet; Point 3 at the FPC collectors outlet; Point 4 at the evaporator outlet (on the normal condition of irradiation); and Point 5 at the turbine outlet. The points being referred to in Fig. 2 are placed in Fig. 1 with circles outside the numbers (with the exception of 2′). The reversible process of pressurization or expansion are described by 2 s or 5s respectively. Formulas for heat transfer and power conversion are developed below.
Enthalpy at Point 2′ is calculated by the following:

$$h_{2'} = h_2 + [h_5 - h_{6(T_6=T_2)}] \cdot \varepsilon_r \tag{1}$$

Where ε_r is the regenerator efficiency. Enthalpy at Point 6 is assigned by assuming $T_6 = T_2$.
Total heat transferred to organic fluid from the collectors is calculated by the following:

$$Q = h_4 - h_{2'} \tag{2}$$

Power generated by the turbine (Eq.3) and that consumed by Pump 1 (Eq.4) are calculated by the following:

$$\begin{aligned} W_t &= (h_4 - h_5) \\ &= \varepsilon_t (h_4 - h_{5s}) \end{aligned} \tag{3}$$

$$\begin{aligned} W_{p,1} &= (h_2 - h_1) \\ &= v_1 (p_2 - p_1) / \eta_p \end{aligned} \tag{4}$$

Meanwhile, net power is calculated by the following:

$$W_{orc} = W_t \cdot \varepsilon_g - W_{p,1} - W_{p,2} \tag{5}$$

In case the negative effect of Pump 2 is considered, calculation of required power $W_{p,2}$ is presented in the following section. Practical ORC efficiency is calculated by the following:

$$\eta_{orc} = \frac{W_{orc}}{Q} \tag{6}$$

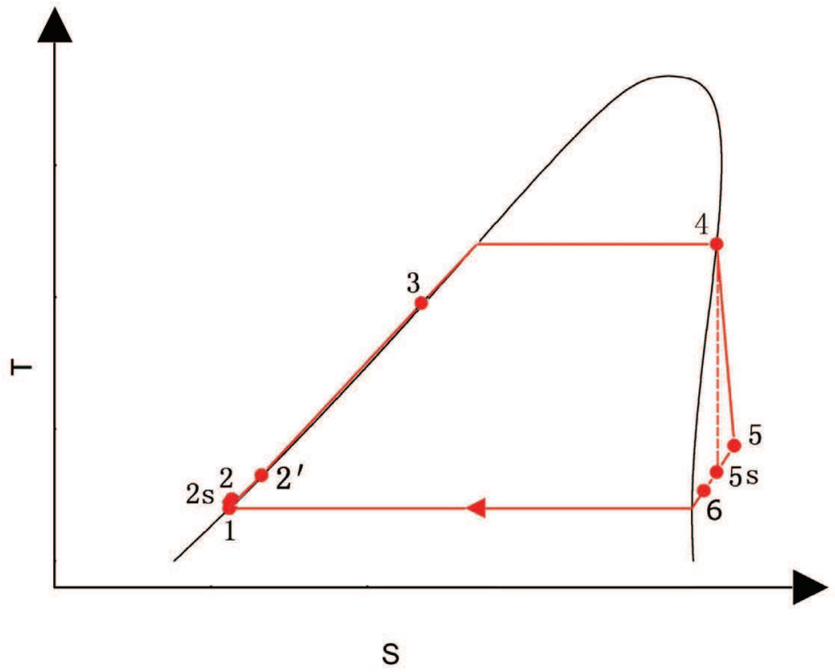

Fig. 2. Thermodynamic cycle of a typical dry fluid

4.2 Equations developed for total thermal efficiency of the collector system

The FPC or CPC collector module available in the market has an effective area of approximately 2.0 m^2 . Its thermal efficiency can be expressed by the following equation:

$$\eta = \eta_0 - \frac{A}{G}(T - T_a) - \frac{B}{G}(T - T_a)^2 \tag{7}$$

Solar thermal electric generation system may demand tens or hundreds of collectors in series, and the temperature differences between neighboring collectors will be small. Thus, it is reasonable to assume the following: 1) the average operating temperature of the collector changes continuously from one module to anther module; and 2) the function of the simulated area of the collector system is integrable.

With inlet temperature T_i and outlet temperature T_o, the required solar collection area is obtained by the following [12]:

$$S = \int_{T_i}^{T_o} \frac{mC_p(T)}{\eta(T)G} dT \tag{8}$$

Temperature of conduction oil in the CPC changes within a small range. This is discussed further in Section 5.2. Heat capacity can be well approximated by the following [16]:

$$C_p(T) = C_{p,0} + \alpha(T - T_0) \tag{9}$$

In the case of FPCs, organic fluid is preheated in low temperature ranges and the first-order approximation of heat capacity can be used as well.

With $c_1 = A / G$, $c_2 = B / G$, the collection area according to Eqs. 8 and 9 is integrated by the following:

$$S = \frac{m}{c_2 G(\theta_2 - \theta_1)}\left[(C_{p,a} + \alpha\theta_1)\ln\frac{T_o - T_a - \theta_1}{T_i - T_a - \theta_1} + (C_{p,a} + \alpha\theta_2)\ln\frac{\theta_2 - T_i + T_a}{\theta_2 - T_o + T_a}\right] \tag{10}$$

where θ_1 and θ_2 are the arithmetical solutions of the following equations ($\theta_1 < 0$, $\theta_2 > 0$).

$$\eta_o - c_1\theta - c_2\theta^2 = 0\ . \tag{11}$$

$$C_{p,a} = C_{p,0} + \alpha(T_a - T_0) \tag{12}$$

Subsequently, total thermal efficiency of the collector system is calculated using the following:

$$\eta_c = \frac{m}{GS}\int_{T_i}^{T_o} C_p(T)dT \tag{13}$$

Combining Eq.13 with Eqs.9 and 10, the following is obtained:

$$\eta_c = \frac{c_2(\theta_2 - \theta_1)[C_{p,0}(T_o - T_i) + 0.5\alpha(T_o - T_i)(T_o + T_i - 2T_0)]}{(C_{p,a} + \alpha\theta_1)\ln\frac{(T_o - T_a - \theta_1)}{T_i - T_a - \theta_1} + (C_{p,a} + \alpha\theta_2)\ln\frac{\theta_2 - T_i + T_a}{\theta_2 - T_o + T_a}} \tag{14}$$

Effect of c_1 is expressed by Eq.11 There are two inlet temperatures, as well as two outlet temperatures in the two-stage collectors. Total collector efficiency is calculated by the following:

$$\eta_c = \frac{Q}{GS} = \frac{\Delta H_1 + \Delta H_2}{\frac{\Delta H_1}{\eta_{FPC}} + \frac{\Delta H_2}{\eta_{CPC}}} \tag{15}$$

where η_{FPC} or η_{CPC} is the first- or second-stage collector efficiency, and ΔH_1 or ΔH_2 is the enthalpy increment of working fluid in the first- or second-stage collectors. The value of $C_{p,0}$ or α or collector heat loss coefficient varies when the fluid or the collector is different.

4.3 Heat transfer between conduction oil and working fluid

Thermal efficiency of FPCs can be calculated directly by the inlet and outlet temperatures of working fluid, according to Eq.14. On the other hand, thermal efficiency of CPC collectors is determined by the heat transfer process in the evaporator. The temperature relationship between working fluid and conduction oil must be established.

This section focuses on heat transfer in the evaporator, and the developed equations can easily be extended to the case of the condenser. Counter-current concentric tubes are adopted, and the parameters are listed in Table 2.

Parameters	Value	Parameters	Value
Outer diameter D_o mm	45	Generator efficiency ε_g	0.95
Inner diameter D_i mm	25	Regenerator efficiency ε_r	0.85
Turbine efficiency ε_t	0.80	Pump efficiency ε_p	0.75
Optical conversion of CPC η_0	0.644	Optical conversion of FPC η_0	0.857
First heat loss coefficient of collectors of CPC A $W/m^{2\,o}C$	0.749	First heat loss coefficient of collectors of FPC A $W/m^{2\,o}C$	3.157
Second heat loss coefficient of collectors of CPC B $W/m^{2\,o}C^2$	0.005	Second heat loss coefficient of collectors of FPC B $W/m^{2\,o}C^2$	0.014

Table 2. Specifications of the proposed low-temperature solar thermal electricity system

The following preconditions are assumed: 1) the influence of pressure drop on the saturated temperature arising from flow resistance in the evaporator is negligible; and 2) the two-phase flow is one-dimensional, that is, all parameters change only in the flow direction (Y).

4.3.1 Liquid-phase region of working fluid

The controlling equations for the energy balance of working fluid and conduction oil are as follows:

$$\frac{dT_f}{dY} = \frac{U\pi D_i(T_h - T_f)}{m_f C_{p,f}} \tag{16}$$

$$\frac{dT_h}{dY} = \frac{U\pi D_i(T_h - T_f)}{m_h C_{p,h}} \tag{17}$$

Total heat transfer coefficient is calculated by the following:

$$U = 1\Big/(\frac{1}{\bar{h}_i} + \frac{1}{\bar{h}_o}) \tag{18}$$

where

$$\bar{h}_i = Nu_f \frac{k_f}{D_i}$$

$$\bar{h}_o = Nu_h \frac{k_h}{(D_o - D_i)}$$

The convectional heat transfer coefficient can be calculated using the Dittus-Boelter equation [17]. When flow of the outer fluid is laminar, the concentric tube is considered isothermal at the inner annulus of the cross-section; it is insulated at the outer annulus, thus obtaining the heat transfer coefficient, according to the *Handbook of Heat Transfer* [18].

4.3.2 Binary-phase region of working fluid

Energy balance of the conduction oil remains to be controlled by Eq.17. However, energy balance (dryness) of organic fluid is controlled by the following:

$$\frac{dx}{dY} = \frac{U\pi D_i (T_h - T_f)}{m_f (h_{f,v} - h_{f,l})} \tag{19}$$

Convection heat transfer coefficient of two-phase flow can be obtained in Rohsenow's handbook [19].

4.4 Calculation of frictional resistance

Viscosity of the oil is generally larger as compared with that of working fluid or water. For precise simulation, flow frictional resistance of oil should be evaluated.
With N lines of the parallel concentric tubes, the required pump power is obtained by the following [17]:

$$W_{oil} \approx \int_{Y1}^{Y2} \frac{128\upsilon \dot{m}^2 \nu}{\pi N (D_o - D_i)^3 (D_o + D_i)\eta_p} dY \tag{20}$$

where $\dot{m}$ is the total mass flow rate of oil through the tubes; υ is the viscosity of oil, $m^2 \cdot s^{-1}$; ν is the specific volume of oil, $m^3 \cdot kg^{-1}$; and $Y2 - Y1$ is the length of a single tube. It is noted that Eq.20 may easily be extended to the case of organic fluid when the negative effect of Pump 2 is considered due to increased flow rate in the evaporator. Subsequently, the properties and diagrams in Eq.20 would be refined.

4.5 Overall thermal efficiency

Net electricity output W is obtained by subtracting oil pump power from net output of the ORC.

$$W = W_{orc} - W_{oil} \tag{21}$$

Global electricity efficiency is defined by the proportion of net electricity output to the total irradiation as follows:

$$\eta = \frac{W}{GS} \tag{22}$$

5. Results and discussion

The parameters for simulation are listed in table 2. The collectors and turbine are key issues of the low temperature solar thermal power system and the performance is proposed according to market available product [20, 21, 22]. The second-stage heat storage medium appropriate for the low temperature solar thermal electric system could be erythritol, which has melting point 120°C and heat of fusion 339.8 kJ/kg. Magnesium chloride hexahydrate ($MgCl_2 \cdot 6H_2O$) would be appropriate as well, which has melting point 117°C, heat of fusion 168.6 kJ/kg and thermal conductivity 0.694 $W/m \cdot K$ (solid). The evaporation temperature considered in this paper is 120°C, which would be well correlated with the above PCMs.

5.1 Comparison of ORC efficiencies

The global efficiency of the proposed system is determined by both heat collection and power conversion processes. In this section, influences of working fluids on the ORC

efficiency are investigated. Performance of working fluids in the ORC is compared in table 3. The environment temperature is 20°C. In order to obtain the same dryness of 1.0 at the evaporator outlet, the collector area for each fluid is different. The state points are referred to as those in the thermodynamic cycle (figure 2). $(h_l - h_{2'}) / (h_4 - h_{2'})$ represents the ratio of heat required in the sub-cooled heating process to the total heat absorbed by fluid in the ORC process. The relationship between this ratio and optimal FPC proportion will be analyzed in Section 5.3.

Table 3 shows that in the case of dry fluids, the regenerator can significantly warm working fluids from the condenser and complement the heat supplied from outside. The temperature arisen in the regenerator for R123, R113, R245fa, pentane or butane is 14.7°C, 23.3°C, 14.2°C, 25.5°C or 15.3°C respectively. The ORC efficiencies of the fluids are close, though R113 has a maximum value of 0.161 and butane has a minimum value of 0.147.

State point		R123	R113	R245fa	pentane	butane
1	t /°C	25	25	25	25	25
	h kJ/kg	225.14	222.67	232.46	-25.93	259.46
2s	t /°C	25.38	25.19	25.60	25.28	25.85
	h kJ/kg	225.89	223.07	233.78	-24.58	262.90
2	t /°C	25.62	25.33	25.93	25.47	26.32
	h kJ/kg	226.14	223.20	234.22	-24.13	264.05
2′	t /°C	40.34	48.46	40.61	50.96	41.58
	h kJ/kg	241.25	244.67	253.79	36.41	301.81
4	t /°C	120	120	120	120	120
	h kJ/kg	449.67	431.71	484.39	490.59	740.69
5s	t /°C	38.52	50.99	40.20	54.81	40.68
	h kJ/kg	406.00	391.45	437.25	392.84	649.49
5	t /°C	50.78	62.71	50.09	65.42	50.48
	h kJ/kg	414.73	399.50	446.68	412.39	667.73
6 assumed	t /°C	25.62	25.33	25.93	25.47	26.32
	h kJ/kg	396.95	374.24	423.66	341.16	623.31
6 real	t /°C	29.46	31.06	29.55	31.69	30.00
	h kJ/kg	399.62	378.03	427.11	351.84	629.97
$(h_l - h_{2'}) / (h_4 - h_{2'})$		0.422	0.377	0.515	0.403	0.514
ORC efficiency		0.154	0.161	0.148	0.160	0.147

Note: h_l is the enthalpy of saturation liquid at 120°C.

Table 3. Comparison of working fluids performance in the ORC

5.2 Heat collection efficiency of single-stage collectors

For the purpose of a better understanding of the advantage of two-stage collectors on heat collection efficiency, a prior study on single-stage collectors is necessary. The collectors in single-stage system and the second stage collectors in two-stage system are CPC collectors connected with evaporator. And single-stage collectors could be interpreted as a special case of two-stage collectors with FPC proportion equal to 0. Heat transfer in the evaporator is simulated in order to establish the relationship between ORC operation temperature and

CPC efficiency. The organic fluid is heated from sub-cooled to binary phase conditions in the evaporator.

Table 4 shows the single-stage collectors efficiency and the specific distribution of thermodynamic parameters. The subscript of f or h represents organic fluid or conduction oil respectively. $x_{f,o}$ is the dryness of organic fluid at evaporator outlet. $T_{f,i}$ is the organic fluid inlet temperature. The evaporator inlet temperatures of the working fluids are different due to the use of regenerator. Since the fluids and conduction oil flow in a contrary direction, the inlet of fluids means location next to the outlet of conduction oil. In order to heat the organic fluid from sub-cooled to saturation vapor state in the evaporator, heat transfer irreversibility between the conduction oil and fluids is large. The average operating temperature of CPC collectors is higher than ORC evaporation temperature, regardless of the much lower inlet temperature of working fluid in the evaporator. A smaller mass flow rate m_h can reduce the outlet temperature of conduction oil $T_{h,o}$, but $T_{h,i}$ will be increased. The reason is that the fluid temperature is constant in the binary phase region and heat is required for evaporation. A smaller m_h would lead to a larger difference between inlet oil temperature and ORC evaporation temperature according to the law of conservation of energy. As collector efficiency declines more steeply at higher operating temperature, small m_h is not preferable.

The heat collection efficiency of single-stage collectors on condition of irradiation 750 W/m^2 for R123, R113, R245fa, pentane or butane is 46.47%, 46.05%, 47.02%, 46.37% or 47.01% respectively.

parameter	Organic fluid				
	R123	R113	R245fa	pentane	butane
m_f kg/s	1.23	1.38	1.12	0.57	0.59
m_h kg/s	7.00	7.00	7.00	7.00	7.00
$T_{f,i}$ °C	40.34	48.46	40.61	50.96	41.58
$x_{f,o}$	1.0	1.0	1.0	1.0	1.0
$T_{h,o}$ °C	116.94	118.61	114.51	117.21	114.43
$T_{h,i}$ °C	133.37	135.15	131.16	133.94	131.32
η_c %	46.47	46.05	47.02	46.37	47.01

Note: irradiation is 750 W/m^2

Table 4. Heat collection efficiency of single-stage collectors

5.3 Influences of working fluids on two-stage collectors

Economical and technological performances as well as collector efficiency have to be taken into consideration to evaluate the low temperature solar thermal power system with two-stage collectors. However, this work is concerned about influences of working fluids on heat collection and power conversion efficiency. In addition to key factors such as irradiation and environmental temperature that affect the efficiency of single-stage collectors, the proportion of FPC area to the total collector area plays an important role in both the overall heat collection efficiency and cost-effectiveness of the two-stage collectors. Figure 3 displays

the heat collection efficiency of two-stage collectors varying with the proportion of FPC area to the total collector area y for each of the working fluids. The environment temperature is 20°C and irradiation is $750\,W/m^2$. The mass flow rates of the fluids are the same as those presented in table 4. The total collector area for each fluid is 690 m^2 and keeps constant when FPC proportion varies. The overall collector efficiency climbs when the FPC area increases in the lower proportion range. However, it drops with further increment of FPC area in the higher proportion range. There exists an optimal FPC proportion y_{opt}, at which the overall collector efficiency reaches the maximum for each fluid. The optimal FPC proportion alters when the working fluid is different.

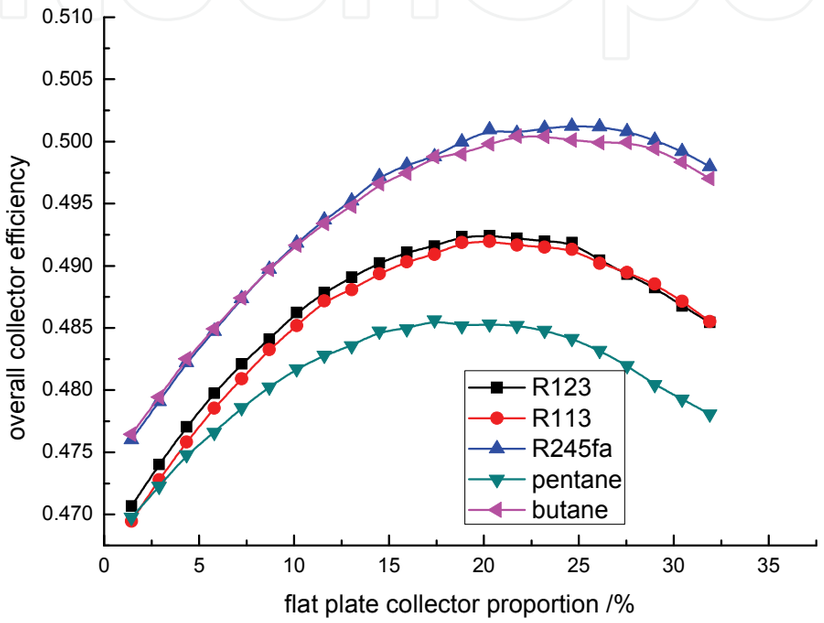

Fig. 3. Heat collection efficiency of two-stage collectors varying with the proportion of FPC area to the total collector area

Table 5 reveals the optimal FPC proportion and the maximum heat collection efficiency variation with working fluids and irradiation. Mass flow rate of each fluid through Pump 1 is equal to that through Pump 2. Thus, the dryness of the working fluids at the evaporator outlet should be 0.5 under normal condition without heat storage or heat release. On the use of Pump 2, superheating is avoidable even if irradiation is strong. Electricity is generated in a wide range of irradiation, and heat transfer between conduction oil and organic fluid is strengthened.

For each fluid, the optimal FPC proportion becomes larger when irradiation is weaker. The decrement of y_{opt} for R123, R113, R245fa, pentane or butane is about 4.2%, 5.5%, 3.9%, 3.1% or 3.0% respectively when irradiation changes from $850\,W/m^2$ to $650\,W/m^2$.

Among the five fluids, R245fa exhibits the highest heat collection efficiency accompanied with the largest FPC proportion. The ratio of heat required in the sub-cooled heating process to the total heat absorbed by fluid in the ORC process $(h_l - h_{2'})/(h_4 - h_{2'})$ for R245fa is the highest as shown in table 3. It seems that the preheating concept of FPC is especially suitable for fluids that have a large heat proportion in the sub-cooled heating process.

Irradiation W/m^2		Organic fluid				
		R123	R113	R245fa	pentane	butane
650	opt. y %	22.1	23.2	25.6	19.5	23.2
	max. $x_{f,o}$	0.347	0.326	0.320	0.334	0.309
	max. η_c %	47.37	47.30	48.33	46.45	48.18
750	opt. y %	18.9	18.8	24.0	17.6	21.7
	max. $x_{f,o}$	0.494	0.459	0.493	0.473	0.479
	max. η_c %	49.23	49.18	50.12	48.56	50.04
850	opt. y %	17.9	17.7	21.7	16.4	20.2
	max. $x_{f,o}$	0.649	0.604	0.672	0.623	0.658
	max. η_c %	50.70	50.56	51.51	50.13	51.41

Table 5. Performance analysis of working fluids on the two-stage collectors

On condition of irradiation of $750\,W/m^2$, the maximum heat collection efficiency for R123, R113, R245fa, pentane or butane is about 49.23%, 49.18%, 50.12%, 48.56% or 50.04% respectively. And the relative increment of heat collection efficiency is 5.94%, 6.80%, 6.60%, 4.73% or 6.45% respectively as compared with that of single-stage collectors (table 4).

6. Conclusion

Heat transfer irreversibility between conduction oil and organic fluids will be large if single-stage collectors are adopted. The low temperature solar thermal electric generation with two-stage collectors and heat storage units gives a flexible system which can react to different operation conditions. Besides, this kind of system displays superior heat collection efficiency as well as cost-effectiveness.

The regenerator can significantly warm working fluids and complement the heat supplied from outside. On the condition of evaporation temperature 120°C, environment temperature 20°C and irradiation $750\,W/m^2$, the ORC efficiency for R123, R113, R245fa, pentane or butane is 0.154, 0.161, 0.148, 0.160 or 0.147 respectively. Although R113 and pentane have the best ORC performance the highest collector efficiency is obtained on the use of R245fa and butane. And the heat collection efficiency is 49.23%, 49.18%, 50.12%, 48.56% or 50.04% respectively. The proportion of FPC area to the total collector area plays an important role in both the overall heat collection efficiency and cost-effectiveness of the two-stage collectors. And the optimal FPC proportion for R123, R113, R245fa, pentane or butane is 18.9%, 18.8%, 24%, 17.6% or 21.7% respectively. In consideration of frictional resistance of conduction oil as discussed in Section 4.4, the global electricity would be about 7.49%, 7.83%, 7.31%, 7.68%, 7.25% respectively.

7. Acknowledgments

This study was supported by the National Science Foundation of China [Project Numbers: 50974150, 50978241 and 50708105] and the National High Technology Research and Development Program of China (863 Program) [Project Number: 2007AA05Z444].

8. References

[1] Prabhu E. Solar trough ORC. Subcontract report NREL/SR-550-39433 (2006)
[2] Rogers G, Mayhew Y. Engineering thermodynamics, work and heat transfer, 4th ed. Harlow: Longman Scientific & Technical; (1992)239–243.
[3] Andersen WC, Bruno TJ. Rapid Screening of Fluids for Chemical Stability in Organic Rankine Cycle Applications. Industrial & Engineering Chemistry Research 44(2005)5560-5566
[4] Sylvain Quoilin, Vincent Lemort. Technological and economical survey of Organic Rankine Cycle systems, 5th European Conference Economics and Management of Energy in Industry, 14-17 April 2009
[5] Tzu-Chen Huang. Waste heat recovery of organic Rankine cycle using dry fluids. Energy Conversion & Management 42(2001)539-553.
[6] Bo-Tau Liu, Kuo-Hsiang Chien, Chi-Chuan Wang. Effect of working fluids on organic Rankine cycle for waste heat recovery. Energy 29(2004)1207-1217.
[7] Bahaa Saleh, Gerald Koglbauer, Martin Wendland, Johann Fischer. Working fluids for low-temperature organic Rankine cycles. Energy 32(2007)1210-1221.
[8] H.D. Madhawa Hettiarachchi, Mihajlo Golubovic, William M. Worek, Yasuyuki Ikegami. Optimum design criteria for an Organic Rankine cycle using low-temperature geothermal heat sources. Energy 32(2007)1698-1706
[9] Drescher and Brueggemann. Fluid selection for the Organic Rankine Cycle (ORC) in biomass power and heat plants. Applied Thermal Engineering 27 (2007) 223–228
[10] X.D. Wang, L. Zhao, J.L. Wang, W.Z. Zhang, X.Z. Zhao, W. Wu. Performance evaluation of a low-temperature solar Rankine cycle system utilizing R245fa. Solar Energy 84 (2010) 353–364
[11] S. Canada, G. Cohen, R. Cable, D. Brosseau, H. Price, Parabolic trough organic Rankine cycle solar power plant, NREL/CP-550-37077, Presented at the 2004 DOE Solar Energy Technologies, Denver, USA, 2004.
[12] Pei Gang, Li Jing, Ji Jie. Analysis of low temperature solar thermal electric generation using regenerative Organic Rankine Cycle. Applied Thermal Engineering 2010; 30: 998–1004.
[13] Li jing, Pei gang, Ji jie. Analysis of key factors in low temperature solar thermal electric power generation with Organic Rankine Cycle. CIESC Journal 60(2009)826-892.
[14] Optimization of low temperature solar thermal electric generation with Organic Rankine Cycle in different areas. Applied Energy (2010), doi:10.1016/j.apenergy.2010.05.013
[15] William Stine, Michael Geyer. Power from the sun, Solar Energy Research Institute, Solar Technical Information Program (U.S.), http://www.powerfromthesun.net/Chapter6/Chapter6.htm
[16] http://www.fiz-chemie.de/infotherm/servlet/infothermSearch
[17] Incropera FP, Dewitt DP, Bergman TL, Lavine AS. Fundamentals of Heat and Mass Transfer. Ge Xinshi; Ye Hong, trans.6th ed. Chemistry Industry Press (Chinese). 2007
[18] Kays W.M, Perkins H.C. Handbook of Heat Transfer. Chapter 7, New York, 1972.
[19] Warren M. Rohsenow, J.P. Hartnett. Handbook of heat transfer, McGraw-Hill, c1973, 14-1
[20] http://www.infinityturbine.com/ORC/ORC_Waste_Heat_Turbine.html

[21] Ritter Solar product CPC 16w OEM, http://www.rittersolar.de
[22] NAU FLATLINE BE Ultra, http://www.ecocalc.com/manufacturer_col/346/Nau+GmbH/FLATLINE+BE+Ultra?ep=1&prid=

Nomenclature

A	First heat loss coefficient, $W \cdot m^{-2} \cdot {}^{o}C^{-1}$
B	Second heat loss coefficient $W \cdot m^{-2} \cdot {}^{o}C^{-2}$
C_p	Heat capacity, $J \cdot kg^{-1} \cdot {}^{o}C^{-1}$
D	Diameter, m
G	Insolation, $W \cdot m^{-2}$
h	Enthalpy, $J \cdot kg^{-1}$
m	Mass ratio, $kg \cdot s^{-1}$
Nu	Nusselt number
p	Pressure, Pa
Q	Heat, $J \cdot kg^{-1}$
S	Collector area, m^2
T	Temperature, ° C
$\overline{h}$	Heat transfer coefficient, $W \cdot m^{-2} \cdot {}^{o}C^{-1}$
v	Specific volume, $m^3 \cdot kg^{-1}$
U	Total heat transfer coefficient, $W \cdot m^{-2} \cdot {}^{o}C^{-1}$
W	Power, $J \cdot kg^{-1}$
x	Dryness
Y	Length, m
y	FPC proportion
	Heat capacity
α	coefficient, $J \cdot kg^{-1} \cdot {}^{o}C^{-2}$
ε	Machine efficiency
η	Efficiency
κ	Conductivity, $W \cdot m^{-1} \cdot {}^{o}C^{-1}$
υ	Viscosity, $m^2 \cdot s^{-1}$
Subscripts	
1-5	State point
a	Environment
c	Collector
f	Organic fluid
g	Generator
h	Conduction oil
i	Inlet
o	Outlet

p	Pump
r	Regenerator
t	Turbine

IntechOpen

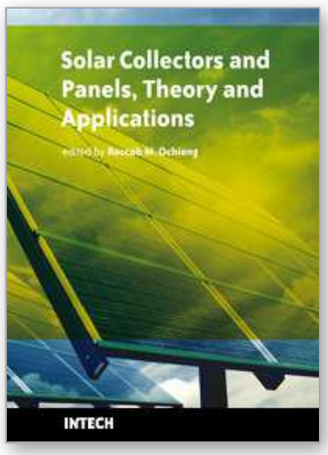

Solar Collectors and Panels, Theory and Applications
Edited by Dr. Reccab Manyala

ISBN 978-953-307-142-8
Hard cover, 444 pages
Publisher Sciyo
Published online 05, October, 2010
Published in print edition October, 2010

This book provides a quick read for experts, researchers as well as novices in the field of solar collectors and panels research, technology, applications, theory and trends in research. It covers the use of solar panels applications in detail, ranging from lighting to use in solar vehicles.

How to reference
In order to correctly reference this scholarly work, feel free to copy and paste the following:

Gang Pei, Jing Li and Jie Ji (2010). Working Fluid Selection for Low Temperature Solar Thermal Power Generation with Two-Stage Collectors and Heat Storage Units, Solar Collectors and Panels, Theory and Applications, Dr. Reccab Manyala (Ed.), ISBN: 978-953-307-142-8, InTech, Available from: http://www.intechopen.com/books/solar-collectors-and-panels--theory-and-applications/working-fluid-selection-for-low-temperature-solar-thermal-power-generation-with-two-stage-collectors

INTECH
open science | open minds

InTech Europe
University Campus STeP Ri
Slavka Krautzeka 83/A
51000 Rijeka, Croatia
Phone: +385 (51) 770 447
Fax: +385 (51) 686 166
www.intechopen.com

InTech China
Unit 405, Office Block, Hotel Equatorial Shanghai
No.65, Yan An Road (West), Shanghai, 200040, China
中国上海市延安西路65号上海国际贵都大饭店办公楼405单元
Phone: +86-21-62489820
Fax: +86-21-62489821

IntechOpen